Search for New Particles at PEP

R. Prepost

Department of Physics, University of Wisconsin, Madison, Wisconsin 53706

ABSTRACT

The status of the search for new particles at the PEP storage ring is reviewed. The primary results presented are based on the TPC search for fractional charges using the dE/dx capability of the time projection chamber and the MAC searches for supersymmetric particle production in both single electron and single photon spectra.

INTRODUCTION

The status of particle searches based on the work of the TPC and MAC groups is presented in this report. The TPC group has extended their search for fractional charges to include a search for 1/3 e and 2/3 e as well as 4/3 e charges. The MAC search for supersymmetric particles based on single electron and single photon spectra is reviewed and the most recent results are presented. A new experiment, now starting to take data at PEP and designed specifically to search for radiative photino pair production is briefly described.

SEARCH FOR FRACTIONAL CHARGES

The TPC group has used the capabilities of the time projection chamber to search for fractional charges. They have previously reported a limit on the production of Q=4/3 e particles[1] and now have the results of a search for the inclusive production of Q=2/3 e and Q=1/3 e particles. All the searches have been done at $\sqrt{s}$=29 GeV. The searches are accomplished by measuring the ionization of tracks with the TPC. Track ionization in the TPC drifts in axial electric and magnetic fields to 12 sectors(6 per endcap) consisting of arrays of proportional wires with 183 wires per sector.[2] Bending plane information is determined from cathode pads located beneath the wires. A schematic view of the TPC is shown in Fig. 1. The new data described here were collected during the spring 1983 running cycle and represent 77 pb^{-1} of integrated luminosity. Multihadron events were identified by requiring five or more verticizing tracks with a total momentum greater than 7.25 GeV/c and a forward backward imbalance of less than 40%. These criteria resulted in a sample of approximately 29K hadronic events.

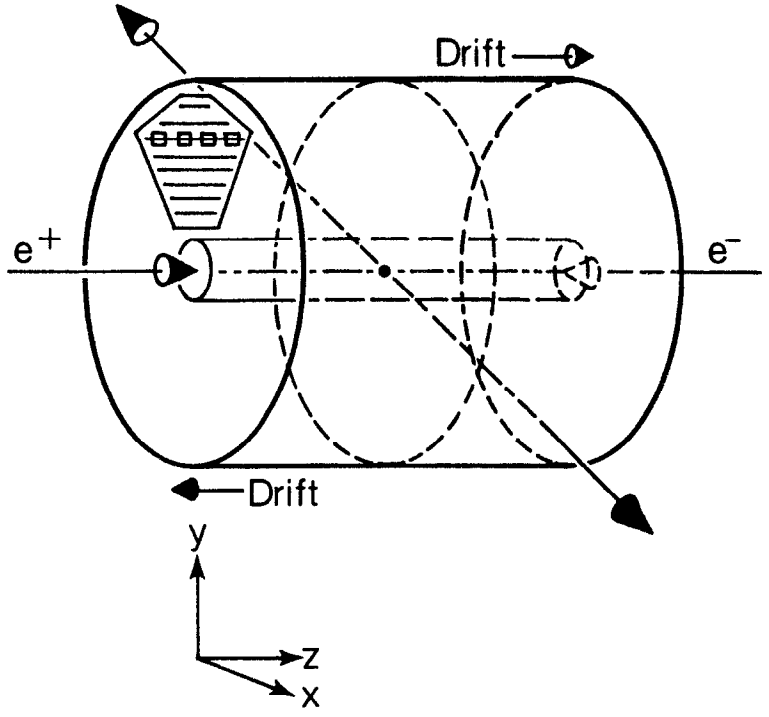

XBL 8310-754A

Fig. 1. Schematic view of the TPC. Track ionization formed in the sensitive volume drifts to arrays of proportional wires. Position in the bending plane is found from signals induced on cathode pads beneath the wires.

The energy loss of a charged particle in a gas scales as $1/\beta^2$ at low velocities, reaches a minimum at $\beta\gamma \approx 3.6$(for the TPC conditions), and then rises logarithmically until it reaches a constant value about 1.4 times the minimum value. In the TPC analysis, $< dE/dx >$ is defined to be the mean of the lowest 65% of the ionization samples collected at the sectors. For this data the TPC had a resolution in $< dE/dx >$ of 3.7% for tracks with at least 80 samples of ionization. Figure 2 shows a scatter plot of $< dE/dx >$ vs measured momentum for a 40% subset of the data. The bands in the figure are due to stable Q=1 particles(e,π,K,p). The figure also shows the curves of $< dE/dx >$ vs apparent momentum for Q=1/3(dashed line) and Q=2/3(solid line) particles with masses of 3 and 10 GeV/c^2 respectively.

The search was performed in regions of $< dE/dx >$ and apparent momentum not populated by stable Q=1 particles. One region is below minimum ionization for Q=1 tracks, and the other is a high apparent momentum and high $< dE/dx >$ region. The low region is bounded by $< dE/dx >$=4.0 KeV/cm and $< dE/dx >$=8.0 KeV/cm. The upper region is bounded by the curve of ionization for 1.8 GeV/c^2 Q=1 particles, by the line corresponding to a $< dE/dx >$ of 40.0 KeV/cm , and by the line corresponding to a $< dE/dx >$ of 24 KeV/cm. Above $< dE/dx >$=40 KeV/cm, electronic saturation becomes a dominant factor, and below $< dE/dx >$=4 KeV/cm particle detection efficiency begins to drop. A region similar to the high $< dE/dx >$ region described above was used for the Q=4/3 e search.

Candidate tracks were selected from the events in the search region with suitable fiducial requirements to stay away from the edges of the sectors. A se-

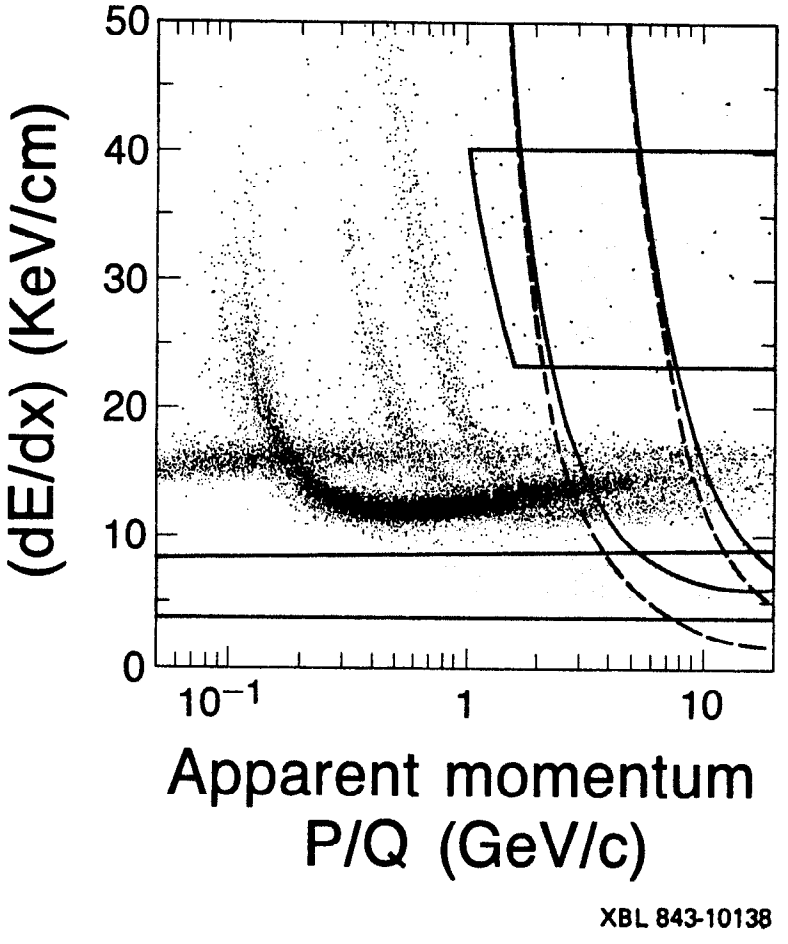

Fig. 2. Scatter plot of $< dE/dx >$ vs apparent momentum (p/Q) for tracks in the data sample. The shaded regions are the search regions defined in the text. The lines are the expected ionization curves for Q=2/3(solid line) and Q=1/3(dashed line) particles with masses of 3 and 10 GeV/c^2.

ries of cuts were also used to eliminate overlapping track pairs as candidates. The above requirements rejected all candidate tracks. Detection efficiencies for the search were determined by a Monte Carlo calculation. The assumed charged particle momentum distributions were taken to be $dN/dp \sim p^2/E$ and $dN/dp \sim (p^2/E)e^{-3.5E}$(E in GeV). The momentum distribution for massive quarks should be similar to the former distribution, and the latter distribution more typical for light quarks, since it models the momentum distribution for the light hadrons. It is also assumed that the quarks do not have larger than normal nuclear cross sections.

The limits on $R_Q = \sigma(e^+e^- \to Q\bar{Q}X)/\sigma(e^+e^- \to \mu^+\mu^-)$ are shown in Figs. 3-5 for Q=4/3, 2/3, and Q=1/3 respectively together with results reported by other groups.

No evidence for the inclusive production of Q=4/3, 2/3, or 1/3 e charges is observed in the search samples. In the mass range of 1-13 GeV/c^2 an upper limit on the ratio R_Q between 4.0×10^{-4} and 5.0×10^{-2} depending on the mass, charge, and production hypothesis has been set.

SEARCHES FOR SUPERSYMMETRIC PARTICLES

1.) Introduction

A search for supersymmetric particle production has been performed using the MAC detector at PEP at $\sqrt{s}$=29 GeV. The reactions which have been studied are: (1) $e^+e^- \to e^{\pm}\tilde{e}^{\mp}\tilde{\gamma} \to e^{\mp}$ and (2) $e^+e^- \to \tilde{\gamma}\tilde{\gamma}\gamma \to \gamma$. The searches involve triggering the detector on either a single electron or a single photon. Reaction 1 is a process for the production of a real single selectron and hence is limited

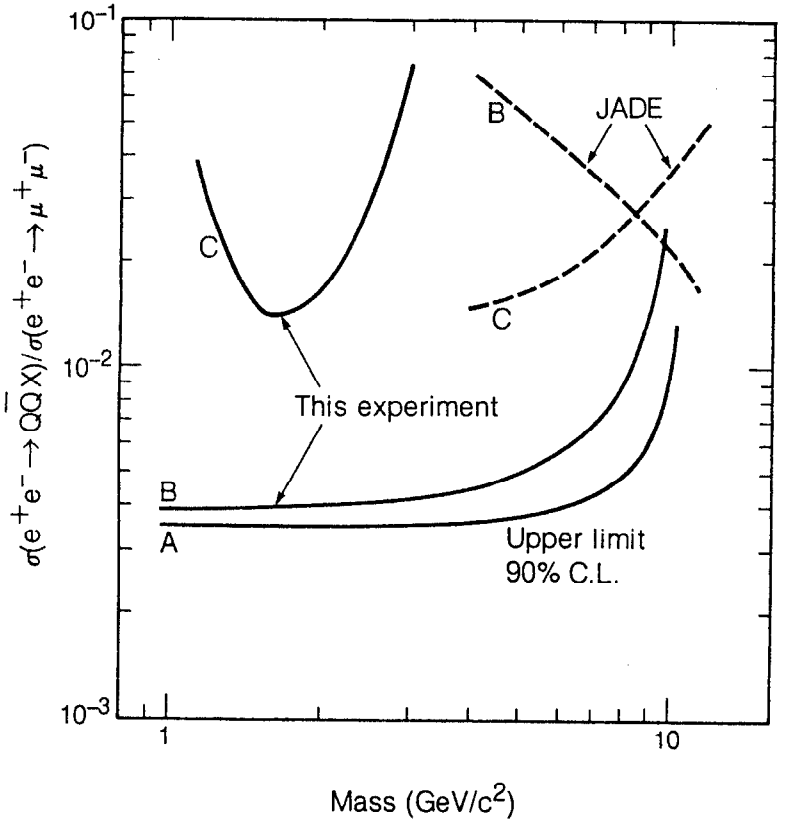

XBL 8310-752

Fig. 3. Limits on the inclusive cross section for Q=4/3 particles. The assumed momentum distributions are: A) $dN/dp \sim (p^2/E)$, B) dN/dp=constant, and C) $dN/dp \sim (p^2/E)e^{-3.5E}$(E in GeV). The solid curves are the limits from this search, the dashed curves are the limits from a search performed by the JADE collaboration.

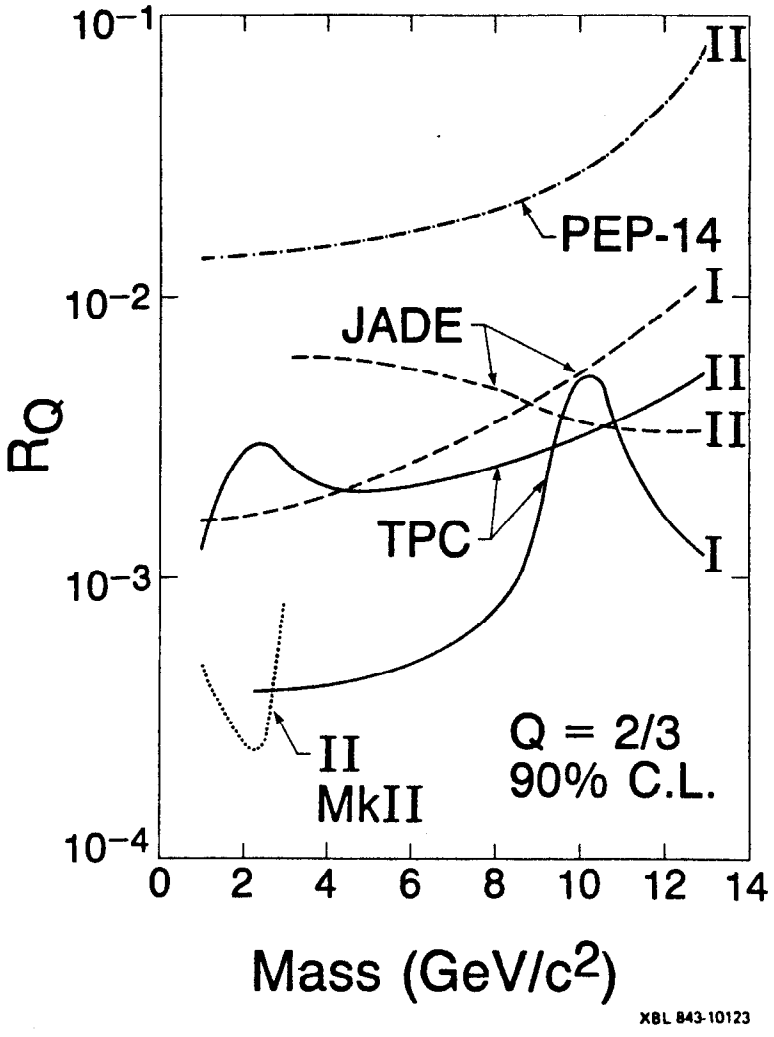

Fig. 4. Upper limit curves(90% CL) for the production of Q=2/3 particles. I.) corresponds to A and II.) corresponds to C in the previous figure. Also plotted are the results of similar searches by the Mark II(dotted line), the JADE group(dashed line), and by the PEP-14 Collaboration(dashed-dotted line).

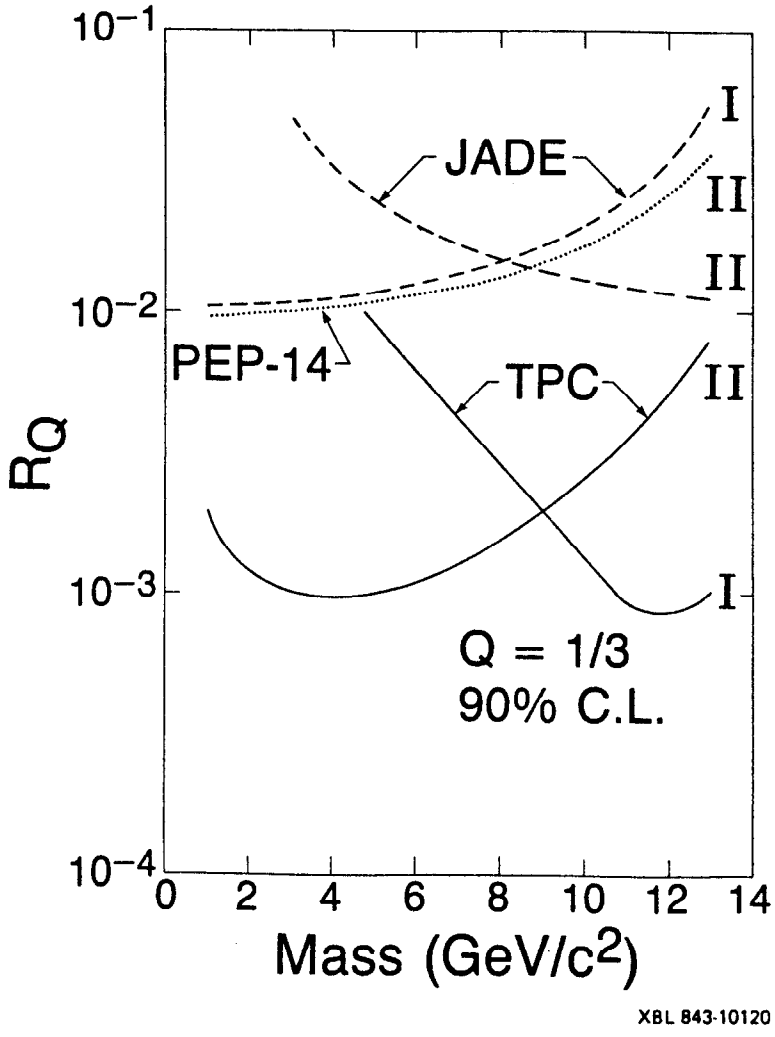

Fig. 5. Upper limit curves(90% CL) for the production of Q=1/3 particles. Also plotted are the results of JADE(dashed line), and by the PEP-14 Collaboration(dotted line). The roman numerals have the same meaning as the previous figure.

to $m_{\tilde{e}} \leq \sqrt{s}$. Reaction 2, on the other hand, is the radiative production of a real photino pair via selectron exchange and hence sets bounds on combinations of the selectron and photino masses. However, for the special case of massless photinos, the limit on the selectron mass is limited only by backgrounds and luminosity and not by the beam energy.

2.) Single $\tilde{e}$ Production

Limits on the selectron mass from Reaction 1 result from an analysis which assumes that the $\tilde{\gamma}$ is stable and not seen in the detector. Calculations for this process[3] also show that the $e^{\pm}$ which accompanies the $\tilde{e}$ in the final state tends to escape undetected down the beam pipe. The only observed final state particle is then the $e^{\mp}$ from the $\tilde{e}^{\mp}$ decay. This electron has high energy $\approx m_{\tilde{e}}/2$ and an almost flat angular distribution. The reaction is sensitive to $m_{\tilde{e}} \leq 2E_{beam}$ depending on the $\tilde{\gamma}$ mass. MAC[4] and MARK II,[5] using this technique, have previously reported lower limits on the $\tilde{e}$ mass of 22.4 and 22.2 GeV/c^2 respectively, at the 95% confidence level. This report updates the MAC search to a data sample three times larger than previously reported.

Background single electron events can come from $ee\gamma$ final states where only one of the electrons is detected. If the detector is inefficient at detecting particles or has dead regions, this background can be several orders of magnitude larger than the expected signal. However, if the undetected particles are constrained to be at small angles relative to the beam axis then momentum conservation limits the energy distribution of the observed electron. A search region for the single electrons can then be defined so that the $ee\gamma$ background is neglible.

More serious backgrounds result from decays of $\tau\tau$, $\tau\tau\gamma$, and $ee\tau\tau$ events in which most of the energy is taken by the neutrinos. If one τ decays to a visible electron and two neutrinos, and the other decays to neutrinos and a soft electron or pion which escapes down the beam pipe, then this event is indistinguishable from the SUSY process. This background has been calculated by Monte Carlo technique.

The MAC detector[6] is well suited for the study of reactions with missing energy and momentum. The detector consists of a cylindrical drift chamber (CD) surrounded by a hexagonal barrel of electromagnetic calorimeters, scintillation counters, and hadronic calorimeters. Planar endcap scintillators and calorimeters extend the coverage to small angles relative to beam. Several layers of drift tubes outside the central and endcap calorimeters provide muon identification and tracking. MAC is essentially 100% efficient for detecting energetic photons and electrons of energy greater than 2 GeV to within $9° - 12°$ of the beam. The detection coverage was extended by the installation of veto calorimeters covering $5° \leq \theta \leq 17°$ during the summer of 1983. Unobserved particles in the $e^+e^-\gamma$ final state are then confined to angles $\leq 5°$. The energy and angular distributions of the observed electron are thus severely restricted by momentum conservation.

The single electron analysis covered two data samples. In the first data sample of 36.4 pb^{-1}, showering particles could be detected to within $9° - 12°$ of the beam. In the second data sample of 77.0 pb^{-1}, taken after the installation of the veto calorimeters, showering particles could be detected to within 5° of the beam. The analysis required a CD track with $|\cos\theta|<0.75$, momentum>1.0 GeV/c, and associated electromagnetic shower energy > 3 GeV (2 GeV for the

second data sample). Events with more than one CD track or shower were rejected, leaving 1565 events from the first data sample. The energy (Fig. 6) and angular distributions of the events from the first data sample are consistent with the expected distributions from $e^+e^- \rightarrow \gamma$ events. The overall trigger and analysis efficiency for the single electron events was calculated to be 92% at 3 GeV and 95% at or above 6 GeV. Electrons produced by $\tilde{e}$ decay are expected to have energies > 8 GeV (see insert in Fig. 6) and thus do not overlap the region populated by the eeγ background.

The energies measured in the veto calorimeters for single electron events in the second data sample are shown in Fig. 7. Events with veto calorimeter energy > 0.25 GeV were rejected as eeγ background. Studies of the veto calorimeter noise indicate that <1.4% of the time $\tilde{e}$ events would fail this cut. The electron energy distribution of the second data sample is seen in Fig. 8. The veto energy cut clearly suppresses the eeγ background. The tail of the the eeγ background is visible for energies below 3 GeV. The remaining events are consistent with τ production processes. In particular, the number of events with electron energy greater than 8 GeV has been estimated to be 0.49±0.06. Utilizing the combined data sample the upper limit on the single electron cross section in the search region is <0.017 pb at the 90% confidence level. As can be seen from Fig. 9, which shows the $\tilde{e}$ cross section in the detector acceptance as a function of mass, the corresponding mass limit is $m_{\tilde{e}} > 25$ GeV/c^2 assuming $m_{\tilde{e}_R} = m_{\tilde{e}_L}$. If $m_{\tilde{e}_L} \gg m_{\tilde{e}_R}$ then the lower limit on the lighter $\tilde{e}$ mass is 24 GeV/c^2. Future increases in the MAC data sample will only marginally improve the $\tilde{e}$ mass limit. Further improvements on the $\tilde{e}$ mass limit will necessarily be made at higher

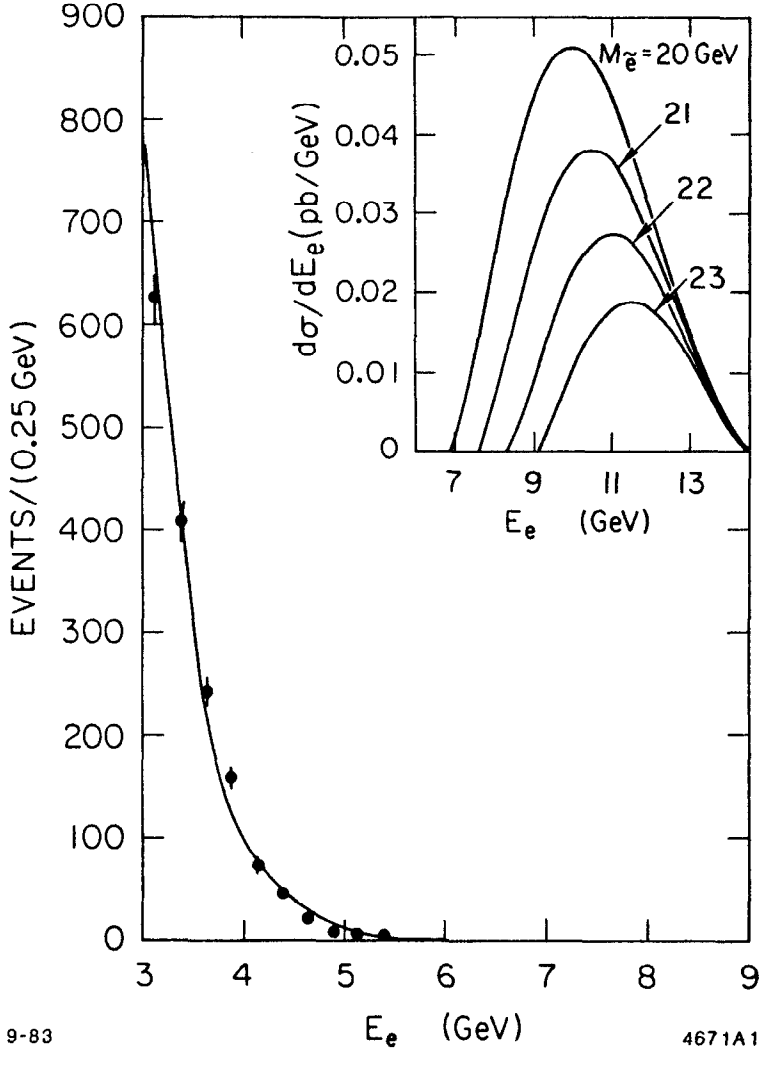

Fig. 6. Energy distribution of single electron events found by MAC in a data sample of 36.4 pb^{-1}. The predicted background from eeγ final states is shown as the solid curve. The expected energy distribution of electrons from $\tilde{e}$ decay is shown in the inset.

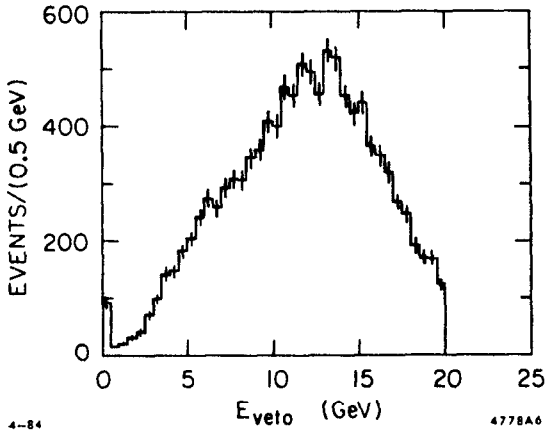

Fig. 7. Energy distribution in the veto calorimeters covering $5° - 17°$ for single electron candidates in a data sample of 29.5 pb^{-1}. Events with $E_{veto} >$ 0.25 GeV were rejected as $ee\gamma$ background.

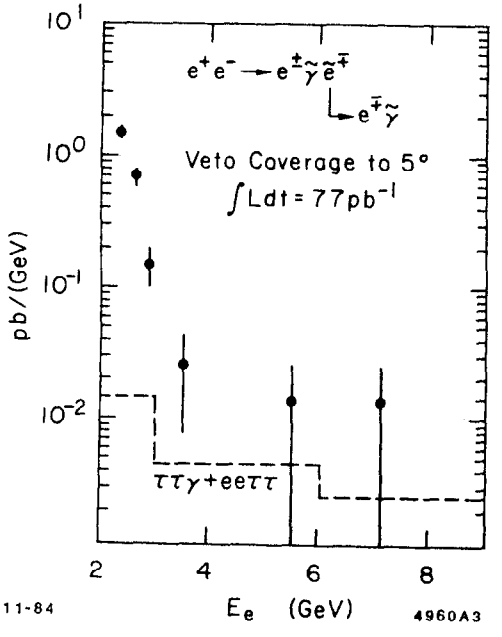

Fig. 8. Electron energy distribution in a data sample of 77 pb^{-1} in which showering particles are detected to within 5° of the beam. The expected energy distribution of electrons from τ production is also shown.

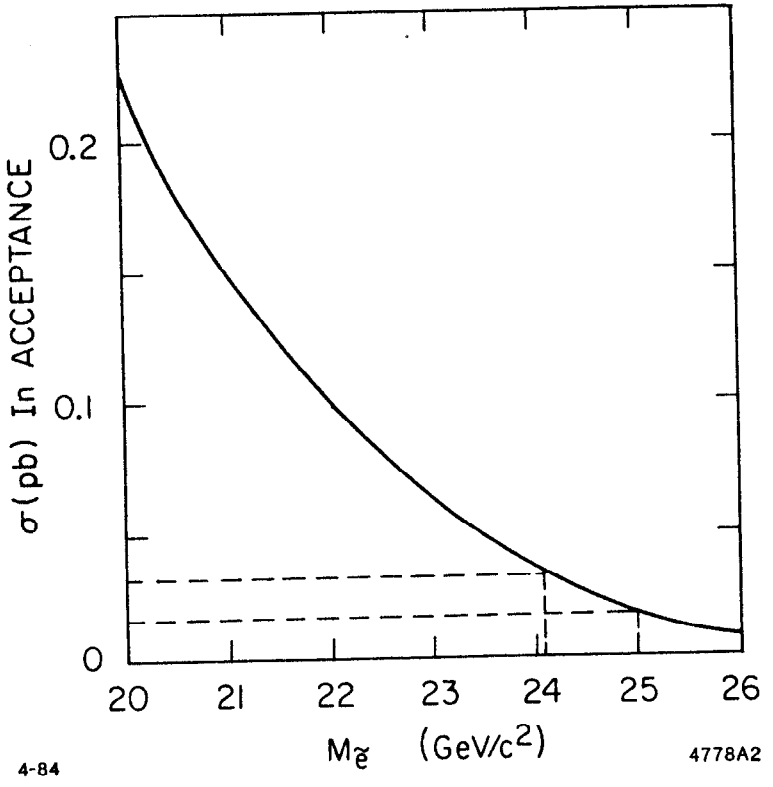

Fig. 9. Cross section in the detector acceptance for electrons from $\tilde{e}$ decays as a function of the $\tilde{e}$ mass. The $\tilde{e}$ mass limits corresponding to the cross section upper limit of 0.017 pb are also shown.

beam energies or with different reactions.

3.) $\tilde{\gamma}$ Pair Production

Reaction 2, $e^+e^- \rightarrow \tilde{\gamma}\tilde{\gamma}\gamma$ involving the detection of a single photon,[7] requires only that the photino is non-interacting in the detector. This reaction also permits $m_{\tilde{\gamma}} = 0$ as a possibility, but in general the mass limits set by the experiment will be a contour with $m_{\tilde{e}}$ and $m_{\tilde{\gamma}}$ as variables.

There are potentially backgrounds to the above process from radiative electromagnetic processes where charged particles are produced at angles smaller than the detector acceptance but where the photon is detected. These backgrounds include radiative Bhabha scattering and radiative tau pair production. The process $e^+e^- \rightarrow \gamma\gamma\gamma$ is a potential background if only one of the photons is emitted into the detector acceptance. There can also be single photons resulting from beam gas interactions and beam spill. Finally, the radiative neutrino pair production process $e^+e^- \rightarrow \gamma\nu\bar{\nu}$ is indistinguishable from the $\gamma\tilde{\gamma}\tilde{\gamma}$ process. However it is very desirable to also measure the cross section for this process. The cross section for radiative photino pair production has been calculated by several authors.[8] The Feynman diagrams which are used for the calculation are shown in Fig. 10 and the cross section for the MAC acceptance is shown in Fig. 11 for several values of the selectron mass. The radiative neutrino pair production cross section is also shown for comparison.[9] At PEP energies, photino production is the dominant process for selectron masses less than about 50 GeV/c^2. The experiment is accomplished by defining acceptance criteria for the detected photon and demanding no other activity in the detector. Since the detector acceptance goes to zero below some minimum angle, this condition corresponds to setting a

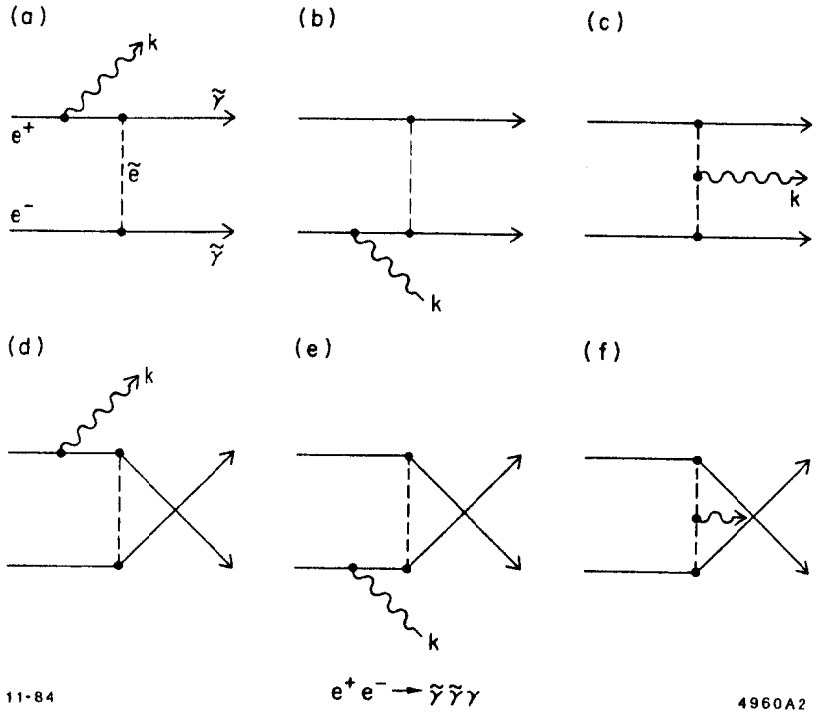

Fig. 10. Feynman diagrams used for the calculation of radiative photino pair production.

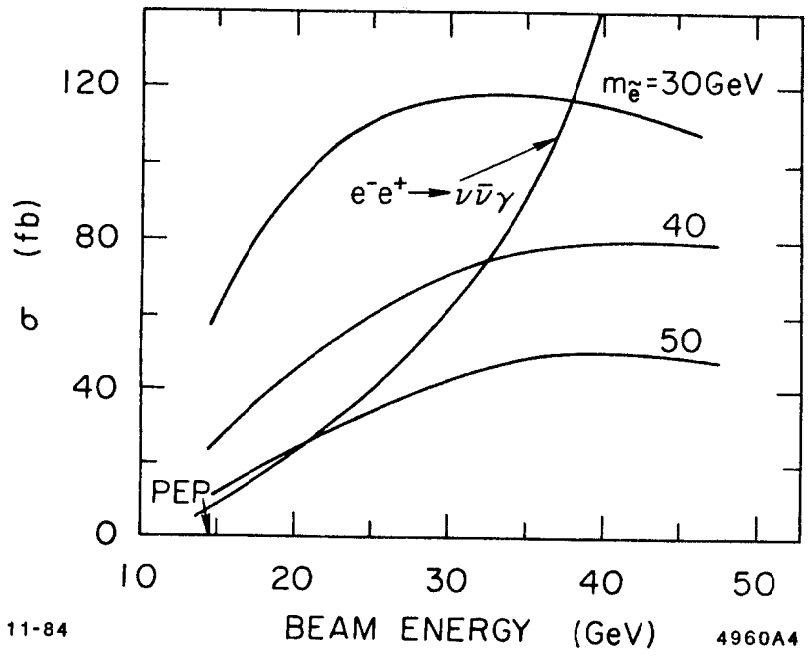

Fig. 11. The radiative photino pair cross section for the MAC acceptance as a function of beam energy for several values of the selectron mass. The radiative neutrino pair cross section is also shown.

minimum veto angle which in turn corresponds to a minimum $E_\perp$ for the detected photon.

The analysis cuts require an electromagnetic shower with $|\cos\theta| < 0.77$ and an energy greater than 1 GeV. Below about 2 GeV the trigger efficiency for single photons begins to fall off. In addition, there can be no charged tracks in the central drift chamber. Further cuts on the electromagnetic shower profile and vertex constraints are also made. These cuts are all tuned experimentally using single electrons and tagged photons from radiative Bhabha scattering.

Two data samples were used for the analysis. For the first data set of 36 pb^{-1} the luminosity and the veto conditions were the same as used for the single $\tilde{e}$ search. The second data set of 80 pb^{-1} was taken after the installation of a special small angle tagging system which covers the region $5° \leq \theta \leq 10°$ with lead-proportional chamber shower counter and lead-scintillator shower counter arrays installed specifically for this experiment. The location of this veto package relative to the main detector is shown in Fig. 12, and the segmentation of the proportional chambers as well as their placement relative to the lead absorber is shown in Fig. 13. The veto calorimeter energy cut was taken to be 0.25 GeV.

The observed $E_\perp$ distibution of the detected photons for the case of the larger($\theta_{veto} \geq 5°$) data sample is shown in Fig. 14 together with the calculated yield from radiative Bhabha scattering. The search regions were taken to be $E_\perp > 4.3$ GeV and $E_\perp > 3.0$ GeV for the two data samples respectively. The overall trigger and analysis efficiencies for the two samples were approximately 65%. The small angle veto inefficiency was determined to be $\approx 10^{-4}$.

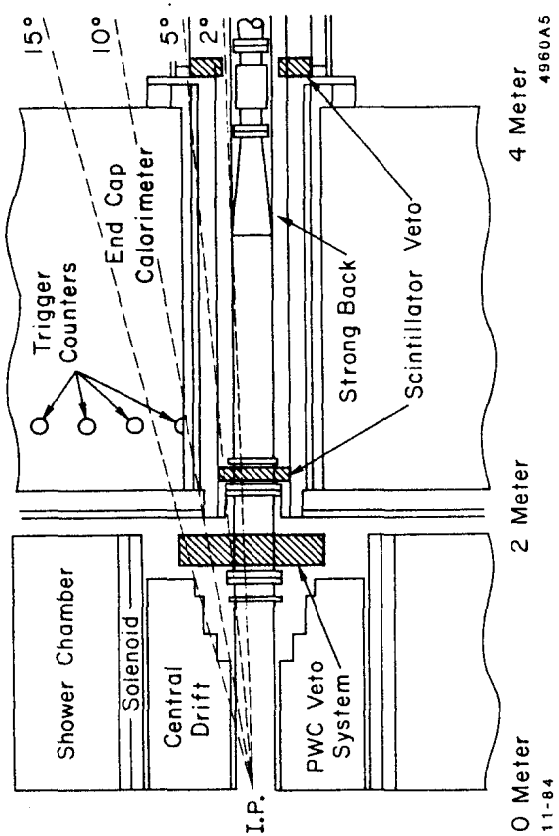

Fig. 12. A schematic drawing of the MAC small angle proportional chamber veto system shown relative to the beam pipe and main detector.

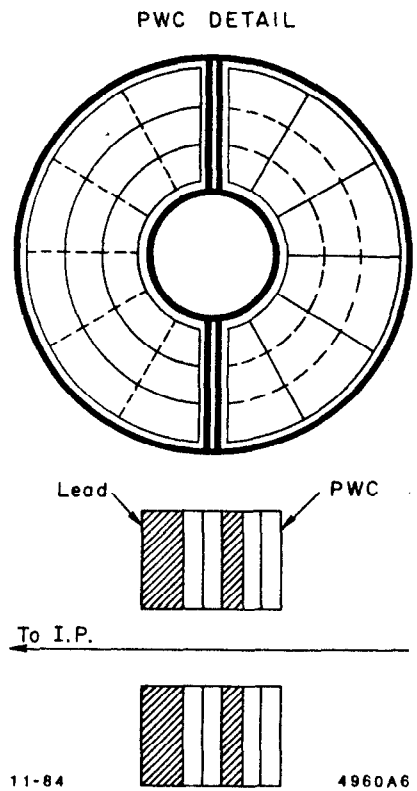

Fig. 13. A detail drawing of the MAC small angle proportional chamber veto system showing the details of the segmentation and the lead packaging.

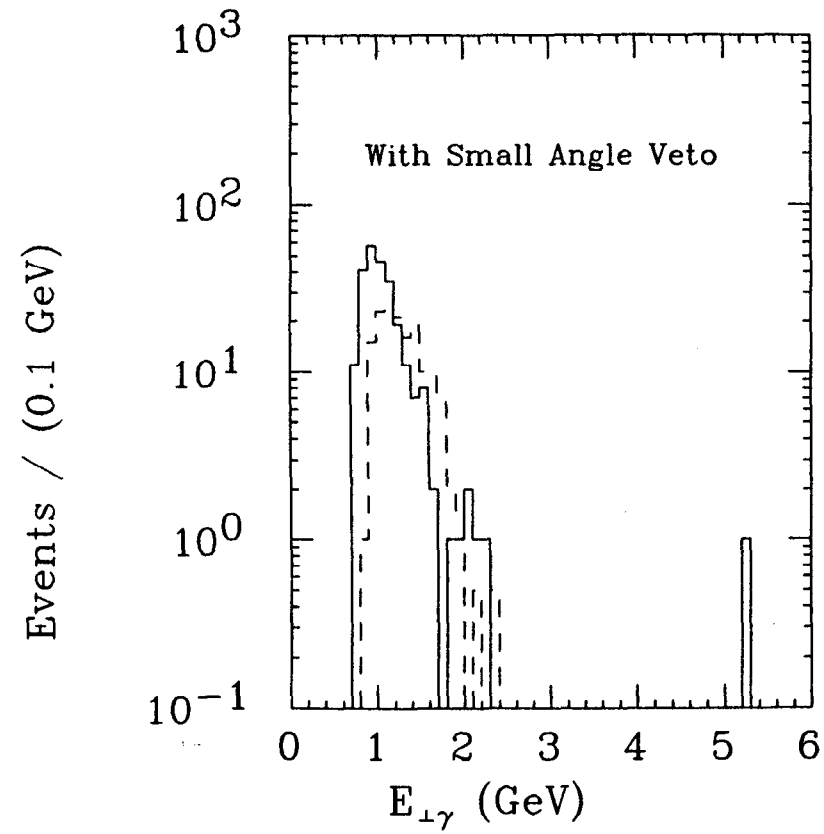

Fig. 14. The observed $E_\perp$ distribution of the detected photons for the case of the 5° minimum angle veto conditions. This is also the larger luminosity sample. The dashed line shows the calculated yield from radiative Bhabha scattering.

The most important backgrounds were calculated to be: $\nu\bar{\nu}\gamma$ ≈0.5 event, $\tau\bar{\tau}\gamma \approx 0.05$ event, and $ee\gamma \approx 0.1$ event. One event is observed in the combined search regions from the second data set at $E_\perp = 5.3$ GeV. If the expected radiative neutrino yield is assumed to be 0.5 event, the 90% confidence level limits obtained for $m_{\tilde{e}}$ and $m_{\tilde{\gamma}}$ are shown in Fig. 15 for $m_{\tilde{e}L} \gg m_{\tilde{e}R}$. The specific case of $m_{\tilde{\gamma}} = 0$ yields:

$$m_{\tilde{e}} > 28.5 \text{ Gev/c}^2 \; for \; m_{\tilde{e}L} \gg m_{\tilde{e}R}$$

and

$$m_{\tilde{e}} > 36.0 \text{ Gev/c}^2 \; for \; m_{\tilde{e}L} = m_{\tilde{e}R}.$$

4.) The ASP Detector

A new detector designed specifically for a single photon search has recently been installed at PEP.[10] This detector, named ASP(anomalous single photons), has been built by a combined SLAC, MIT, Washington, and Fermilab group, and consists of an array of segmented glass blocks and scintillation counters together with a central PWC tracking array and scintillator veto counters surrounding the interaction region. The detector also includes a forward arm shower system with the capability to veto charged particles down to 20 mr. The calculated sensitivity of the detector is such that if no events are found in 100 pb^{-1}, the mass limits for the case of left-right degenerate selectrons will be $m_{\tilde{e}} > 60$-65 GeV/c^2 at the 90% confidence level, and the neutrino number limit will be $N_\nu < 7$. A cross section of the detector is shown in Fig. 16, and Fig. 17 shows a detail of the forward arms.

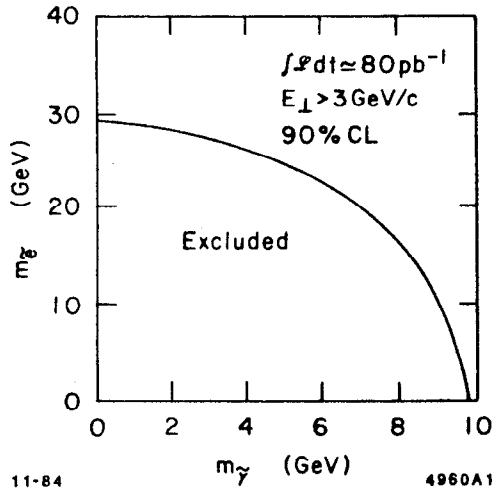

Fig. 15. The 90% confidence level selectron and photino mass limits determined from this experiment for the case $m_{\tilde{e}L} \gg m_{\tilde{e}R}$.

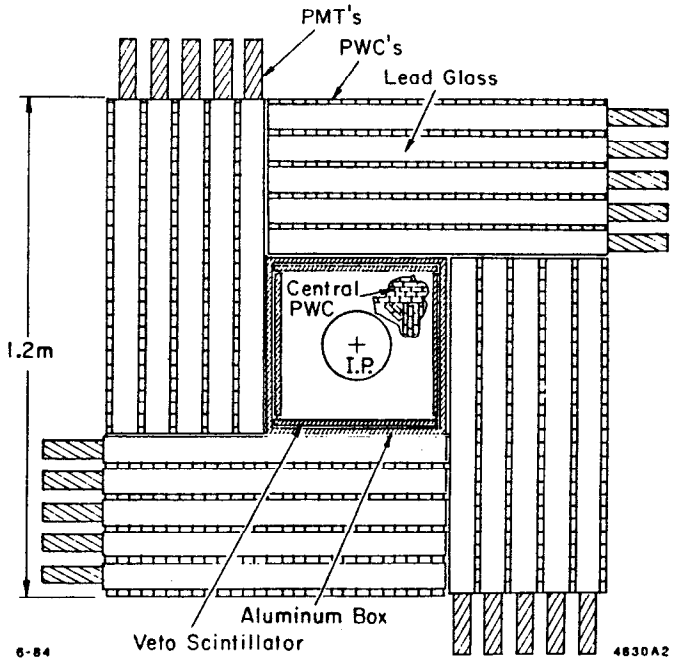

Fig. 16. A schematic drawing of the ASP detector seen along the beam direction.

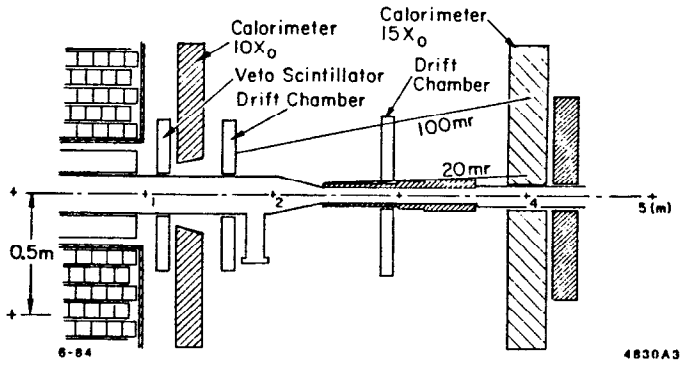

Fig. 17. A schematic detail of the ASP detector showing the forward arms.

This detector is now installed at PEP and has already taken data in 1984 with 50% of the central system and 100% of the forward system in place.

CONCLUSIONS

No evidence of fractional charge or supersymmetric particles has been found by the TPC and MAC detectors. The TPC group has extended the search for fractional charges to 1/3 e and 2/3 e and the results provide the best limits for fractional charge in e^+e^- interactions over most of the range of masses where limits have been set. The MAC group has established a selectron mass limit of 36 GeV/c^2(for $m_{\tilde{\gamma}}$=0) at the 90% confidence level. The search for direct single selectron production gives a similar although smaller mass limit. The prospects are that the selectron mass limits may be increased to the 60 GeV/c^2 level by the ASP detector within the next several years. It is, of course, not out of the question that a real signal may be found.

ACKNOWLEDGEMENTS

I would like to thank my MAC colleagues for their support and tireless efforts to make the MAC detector successful. I would like to thank the TPC collaboration for supplying results and R. Hollebeek of the ASP collaboration for supplying detector information. Finally, I would like to thank the PEP staff for the smooth running and performance which makes for successful experiments.

This work was supported in part by the Department of Energy under contract number DE-AC02-76ER00881.

REFERENCES

1. H. Aihara et al., Phys. Rev. Lett. 52, 168 (1984).
2. H. Aihara et al., IEEE Trans. Nuc. Sci. 30, 63, 76, 162 (1983).
3. M. K. Gaillard, L. Hall, and I. Hinchliffe, Phys. Lett. 116*B*, 279 (1982).
4. E. Fernandez et al., Phys. Rev. Lett. 52, 22 (1984).
5. L. Gladney et al., Phys. Rev. Lett. 51, 2253 (1983).
6. W. T. Ford in *Proceedings of the International Conference on Instrumentation for Colliding Beams,* edited by W. Ash, SLAC report No. SLAC-250, 1982.
7. P. Fayet, Phys. Lett. 117*B*, 460 (1982); J. Ellis and J. S. Hagelin, Phys. Lett. 122*B*, 303 (1983).
8. K. Grassie and P. N. Pandita, Phys. Rev. *D*30, 22 (1984); J. Ware and M. E. Machacek, Phys. Lett. 142*B*, 300 (1984); T. Kobayashi and M. Kuroda, Phys. Lett. 139*B*, 208 (1984).
9. E. Ma and J. Okada, Phys. Rev. Lett. 41, 287 (1978); K. J. F. Gaemers et al., Phys. Rev. *D*19, 1605 (1979).
10. PEP Proposal PEP-21, D.Burke, R. Hollebeek et al., March 1983.